

## Rothamsted Repository Download

### A - Papers appearing in refereed journals

Kong, F. T., Liang, Y. X., Legeret, B., Beyly-Adriano, A., Blangy, S., Haslam, R. P., Napier, J. A., Beisson, F., Peltier, G. and Li-Beisson, Y. 2017. Chlamydomonas carries out fatty acid beta-oxidation in ancestral peroxisomes using a bona fide acyl-CoA oxidase. *The Plant Journal*. 90 (2), pp. 358-371.

The publisher's version can be accessed at:

- <https://dx.doi.org/10.1111/tpj.13498>

The output can be accessed at: <https://repository.rothamsted.ac.uk/item/8v49q>.

© 31 January 2017, Wiley-Blackwell.

# *Chlamydomonas* carries out fatty acid $\beta$ -oxidation in ancestral peroxisomes using a bona fide acyl-CoA oxidase

Fantao Kong<sup>1</sup>, Yuanxue Liang<sup>1</sup>, Bertrand Légeret<sup>1</sup>, Audrey Beyly-Adriano<sup>1</sup>, Stéphanie Blangy<sup>1</sup>, Richard P. Haslam<sup>2</sup>, Johnathan A. Napier<sup>2</sup>, Fred Beisson<sup>1</sup>, Gilles Peltier<sup>1</sup> and Yonghua Li-Beisson<sup>1,\*</sup>

<sup>1</sup>Commissariat à l'Energie Atomique et aux Energies Alternatives, CNRS, Aix Marseille Université, UMR7265, Institut de Biosciences et Biotechnologies Aix Marseille, 13108 Cadarache, France, and

<sup>2</sup>Department of Biological Chemistry and Crop Protection, Rothamsted Research, Harpenden, UK

Received 9 September 2016; revised 25 January 2017; accepted 27 January 2017; published online 31 January 2017.

\*For correspondence (e-mail yonghua.li@cea.fr).

## SUMMARY

Peroxisomes are thought to have played a key role in the evolution of metabolic networks of photosynthetic organisms by connecting oxidative and biosynthetic routes operating in different compartments. While the various oxidative pathways operating in the peroxisomes of higher plants are fairly well characterized, the reactions present in the primitive peroxisomes (microbodies) of algae are poorly understood. Screening of a *Chlamydomonas* insertional mutant library identified a strain strongly impaired in oil remobilization and defective in *Cre05.g232002* (*CrACX2*), a gene encoding a member of the acyl-CoA oxidase/dehydrogenase superfamily. The purified recombinant CrACX2 expressed in *Escherichia coli* catalyzed the oxidation of fatty acyl-CoAs into *trans*-2-enoyl-CoA and produced H<sub>2</sub>O<sub>2</sub>. This result demonstrated that CrACX2 is a genuine acyl-CoA oxidase, which is responsible for the first step of the peroxisomal fatty acid (FA)  $\beta$ -oxidation spiral. A fluorescent protein-tagging study pointed to a peroxisomal location of CrACX2. The importance of peroxisomal FA  $\beta$ -oxidation in algal physiology was shown by the impact of the mutation on FA turnover during day/night cycles. Moreover, under nitrogen depletion the mutant accumulated 20% more oil than the wild type, illustrating the potential of  $\beta$ -oxidation mutants for algal biotechnology. This study provides experimental evidence that a plant-type FA  $\beta$ -oxidation involving H<sub>2</sub>O<sub>2</sub>-producing acyl-CoA oxidation activity has already evolved in the microbodies of the unicellular green alga *Chlamydomonas reinhardtii*.

**Keywords:** acyl-CoA oxidase, microbodies, lipid catabolism, oil content, hydrogen peroxide, lipid homeostasis, nitrogen starvation, catalase, lipid droplet, *Chlamydomonas reinhardtii*.

## INTRODUCTION

The  $\beta$ -oxidation of fatty acids (FAs) plays a pivotal role in eukaryotic cells. This catabolic pathway generates acetyl-CoAs via breakdown of FAs acquired from the environment or released upon hydrolysis of membrane structural lipids and storage triacylglycerols (TAGs) by lipolytic enzymes (lipases), and could also be de novo synthesized FAs when the rate of synthesis bypass downstream metabolic needs (Marchesini and Poirier, 2003; Poirier *et al.*, 2006; Graham, 2008). Lipid degradation therefore provides cells with carbon skeletons and energy to drive anabolic processes whilst also ensuring membrane function and cell fitness through the elimination of oxidized, toxic or unusual FAs produced either after being exposed to adverse growth conditions or via transgenic means (Marchesini and Poirier, 2003; Moire *et al.*, 2004; Poirier *et al.*, 2006; Napier, 2007). Lipid catabolic processes and the enzymes involved

have been studied intensively in mammalian cells (Eaton, 2002), in germinating oilseeds (Graham, 2008) and in fungal species that can utilize FAs as a carbon source (Daum *et al.*, 2007), and have also recently been explored in plant leaves (Kunz *et al.*, 2009; Troncoso-Ponce *et al.*, 2013; Fan *et al.*, 2014). In mammalian cells  $\beta$ -oxidation of FAs occurs in both mitochondria and peroxisomes (Eaton, 2002), but in plant/fungal cells it occurs exclusively in the peroxisome (Purdue and Lazarow, 2001; Poirier *et al.*, 2006; Graham, 2008).

Peroxisomes (also called microbodies) are small single membrane-bound entities, and were originally defined as organelles that carry out oxidative reactions leading to the production of hydrogen peroxide (H<sub>2</sub>O<sub>2</sub>); thus the occurrence of peroxisomes allows the separation of otherwise dangerous oxidative reactions from the remaining cellular

metabolism. Since the discovery of peroxisomes in the 1950s (Rhodin, 1954), the metabolic processes occurring within them have been well studied in a few model organisms including human and *Saccharomyces cerevisiae* (Purdue and Lazarow, 2001), *Pichia pastoris* (Gasser *et al.*, 2013), *Yarrowia lipolytica* (Ledesma-Amaro and Nicaud, 2016) and the higher plant *Arabidopsis thaliana* (Poirier *et al.*, 2006; Graham, 2008; Hu *et al.*, 2012).

Plant peroxisomes are the best characterized in the green lineage, and are known to perform a plethora of functions including lipid metabolism, detoxification, nitrogen metabolism, photorespiration and synthesis of some hormones (Kaur *et al.*, 2009; Hu *et al.*, 2012). Most of the metabolic processes in the peroxisome are a part of large metabolic networks spanning several other subcellular organelles, notably plastids and mitochondria. Indeed, physical associations of peroxisomes with mitochondria or plastids have been observed in 7-day-old *Arabidopsis* seedlings under transmission electron microscopy (Kaur *et al.*, 2009). Essential roles of peroxisomes in coordinating plant metabolism can also be seen through their dynamic nature (increases in both size and number), and that plants without peroxisomes are not viable (Kaur *et al.*, 2009; Hu *et al.*, 2012). Moreover, the peroxisome has been shown to be useful target for re-programming plant metabolism to produce bioplastics and to increase plant biomass productivity (Poirier, 2002; Moire *et al.*, 2004; Poirier *et al.*, 2006; Kessel-Vigeli *et al.*, 2013).

Despite the essential functions attributed to peroxisomes in higher plants, and the growing interest in microalgae for green biotechnology, little is known about the metabolic repertoire of algal peroxisomes or about degradation of FAs in microalgae. Earlier literature suggests that, depending on algal species, FA degradation can occur in mitochondria, in peroxisomes or in both organelles (Stabenau *et al.*, 1984, 1989; Winkler *et al.*, 1988). Differences in the compartmentalization of the enzymes of the FA oxidative pathway have been suggested as a consequence of different phylogenetic development. Of particular note, it is reported that a few algal species in the genera *Mougeotia*, *Pyramimonas* and *Eremosphaera* harbor a peroxisomal acyl-CoA oxidizing (ACX) enzyme which uses O<sub>2</sub> as an electron acceptor and produces H<sub>2</sub>O rather than H<sub>2</sub>O<sub>2</sub> (Winkler *et al.*, 1988; Stabenau *et al.*, 1989). This feature is often observed in peroxisomes that lack catalase (Stabenau *et al.*, 1989). Thus certain algal species may harbor ACXs with activities different from the H<sub>2</sub>O<sub>2</sub>-producing ones present in higher plants.

In this study, we used the green unicellular microalga *Chlamydomonas reinhardtii* as a model to uncover factors involved in lipid hydrolysis. To this end, we employed a forward genetic approach to screen for mutants compromised in oil remobilization. We report here the detailed genetic, biochemical and cell biological characterization of a mutant defective in a member of the acyl-CoA oxidase/

dehydrogenase superfamily. We show that this protein encodes an enzyme with a genuine acyl-CoA oxidase activity (producing H<sub>2</sub>O<sub>2</sub>) that is required for breakdown of FAs during lipid remobilization. We provide experimental evidence for the physiological roles of FA  $\beta$ -oxidation in algal diurnal growth. Finally we demonstrate that shutting down core enzymes of the FA  $\beta$ -oxidation spiral increases oil content in green microalgae.

## RESULTS

### Isolation of a *Chlamydomonas* mutant compromised in oil degradation

To understand lipid turnover processes in green microalgae, we screened an insertional mutant library for strains perturbed in their capacity to remobilize oil reserves. The screening procedure has previously been described in detail (Cagnon *et al.*, 2013). Briefly, cells were cultivated in acetate-containing medium (TAP) and then boosted to accumulate oils via removal of nitrogen (N; TAP-N72 h). In the wild-type (WT) strains oil is usually used rapidly to power regrowth upon resupply of N (Siaut *et al.*, 2011). Oil content was determined 24 h after addition of N back to the culture (MM24h). Several mutants were found to be impaired in their capacity to remobilize oil upon N resupply, including *Nb7D4* (Figure 1a,b). Oil quantification based on densitometry showed that in this mutant 50–70% of oils accumulated at the height of the oil accumulation phase were retained in the mutant 24 h after N resupply when kept in the dark, contrasting with WT cells where 20–30% of oil is retained (Figure 1c). The retention of oils in the lipid droplet (LD) was observed using confocal microscopy (Figure 1d). Flow cytometry, chemical lipid analysis and microscopy therefore pointed to a severe defect in oil degradation in the *Nb7D4* mutant.

### *Nb7D4* is disrupted in *Cre05.g232002* encoding an acyl-CoA oxidase (ACX)

The insertion site of the paromomycin resistance gene (*AphVIII*) in *Nb7D4* was identified by restriction enzyme site-directed amplification (RESDA)-PCR (Gonzalez-Balaster *et al.*, 2011). Using a combination of specific and degenerate primers, a fragment of 1000 bp was amplified, including 426 bp of the *AphVIII* gene and 574 bp of flanking sequences. The fragment was sequenced and then Blasted against the genome of *C. reinhardtii* v5.5 (Phytosome); *AphVIII* was found inserted in the third intron of the locus *Cre05.g232002* (Figure 2a). A RT-PCR analysis using gene-specific primers demonstrated that the insertion resulted in null expression of *Cre05.g232002* in the mutant background (Figure 2b). *Cre05.g232002* encodes a protein of 76 kDa and is annotated as acyl-CoA oxidase in v5.5 of the *C. reinhardtii* genome (Merchant *et al.*, 2007). In many organisms, acyl-CoA oxidase (EC1.1.1.3) catalyzes the first

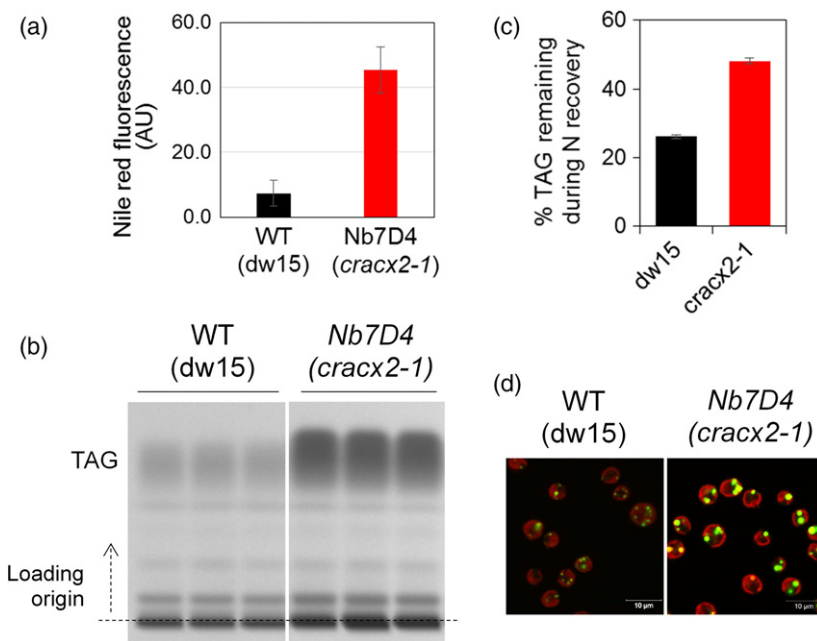


**Figure 1.** The mutant *Nb7D4* (*cracx2*) is compromised in oil turnover.

(a) Oil content screening by flow cytometry based on Nile red fluorescence.

(b) Chemical quantification of oil content by thin layer chromatography (TLC).

(c) Defect in triacylglycerol (TAG) remobilization. Cells were starved nitrogen for 3 days, and samples were taken for analysis during the recovery phase (+N24 h). Each lane represents one biological replicate from that genotype. Total lipids were extracted from a fixed number of cells, then deposited onto a TLC plate, and TAGs were revealed after staining with a  $\text{CuSO}_4$  containing solution (see Experimental procedures for details). This is a representative of at least four or six biological replicates done at different times. Error bars represent standard deviation.

(d) Retention of lipid droplet in the mutant cells as revealed by staining with Nile red.

Lipid droplets are colored green and chlorophyll autofluorescence is in red. Bars = 10 μm. AU, artificial unit. [Colour figure can be viewed at [wileyonlinelibrary.com](http://wileyonlinelibrary.com)].

committed step in FA  $\beta$ -oxidation, thus exerting major control on this pathway (Klein *et al.*, 2002; Haddouche *et al.*, 2010; Theodoulou and Eastmond, 2012). BlastP analysis of this protein on The Arabidopsis Information Resource (TAIR) website revealed that its amino acid sequence is mostly similar to Arabidopsis AtACX2 (At5g65110) (54% identity, and 68% similarity). Based on this sequence homology, we named the protein encoded by the locus *Cre05.g232002* as CrACX2, and the mutant *Nb7D4* as *cracx2-1*.

#### Genetic complementation and isolation of a second allele of the mutant *cracx2-2*

To confirm that the *cracx2-1* mutant phenotype was a result of the disruption of the gene *Cre05.g232002*, complementation of the mutant with a cDNA of the WT locus *Cre05.g232002* was conducted. To this, we first cloned the full-length transcript (2025 bp; corresponding to *Cre05.g232002.t2.1*) into the vector pChlamy4 in frame to the 3' end of the epitope V5. Despite several trials, we could not clone the cDNA corresponding to *Cre05.g232002.t1.1*. The promoters and gene structure information are shown in Figure S1(a) in the Supporting Information. After screening about 100 independent zeocin-resistant clones, one clone (*cracx2-1*;V5-CrACX2) recovered almost its full capacity to remobilize oil (Figure 2c), and the presence of the expressed protein is validated by immunoblot against the anti-V5 antibodies (Figure 2d). Results for some representative clones possessing varying degrees of complementation are shown in Figure S2. Due to the notorious low expression of transgenes in the nuclear genome of *C. reinhardtii*, only a few complemented lines were obtained here.

A second allele (LMJ.SG0182.014586) was identified in the mutant library made by the Jonikas group (Li *et al.*, 2016). It harbors an insertion in the first intron (Figure 2a). The null expression of *CrACX2* in this mutant was confirmed by RT-PCR (Figure 2b). Analyses of oil content during the N recovery phase showed impairment in oil remobilization, i.e. the same defect as observed for the *cracx2-1* mutant (Figure 2e). We thus named this line *cracx2-2*. Dynamic changes in TAG content in both mutant alleles (*cracx2-1*, *cracx2-2*) and their corresponding WT strains are shown in Figure S3. Taken together, these data firmly establish that the impairment in oil remobilization in the mutants is due to disruption in the normal expression of *CrACX2*.

#### *cracx2* is defective in $\beta$ -oxidation of FAs

To determine if the failure of *cracx2* to utilize TAG is caused by impaired  $\beta$ -oxidation, we tested the growth of *Chlamydomonas* on minimal medium (MM) containing oleic acid as the sole carbon source in the dark. Indeed, *Chlamydomonas* cells are able to utilize oleic acid supplied in the medium to drive TAG synthesis in the presence of light and acetate (Fan *et al.*, 2011). The utilization of oleic acid as a source of carbon requires a functional  $\beta$ -oxidation cycle in which oleic acid is reduced to acetyl-CoA then to sugars through the glyoxylate and gluconeogenesis pathways (Graham, 2008). We reasoned that mutants defective in the  $\beta$ -oxidation of FAs should display reduced growth when cultivated in the presence of oleic acid as the only carbon source.

To test this, cells were grown under strict photoautotrophic conditions, transferred to oleic acid-

**Figure 2.** Nb7D4 is defective in an acyl-CoA oxidase.

(a) The insertion site of the cassette *AphVIII* in the mutant *Nb7D4* (*cracx2-1*), and in the second line *cracx2-2* (background strain CC-4533), respectively.

(b) RT-PCR valid zero expression of *CrACX2* in the *cracx2-1* and *cracx2-2* mutants, respectively.

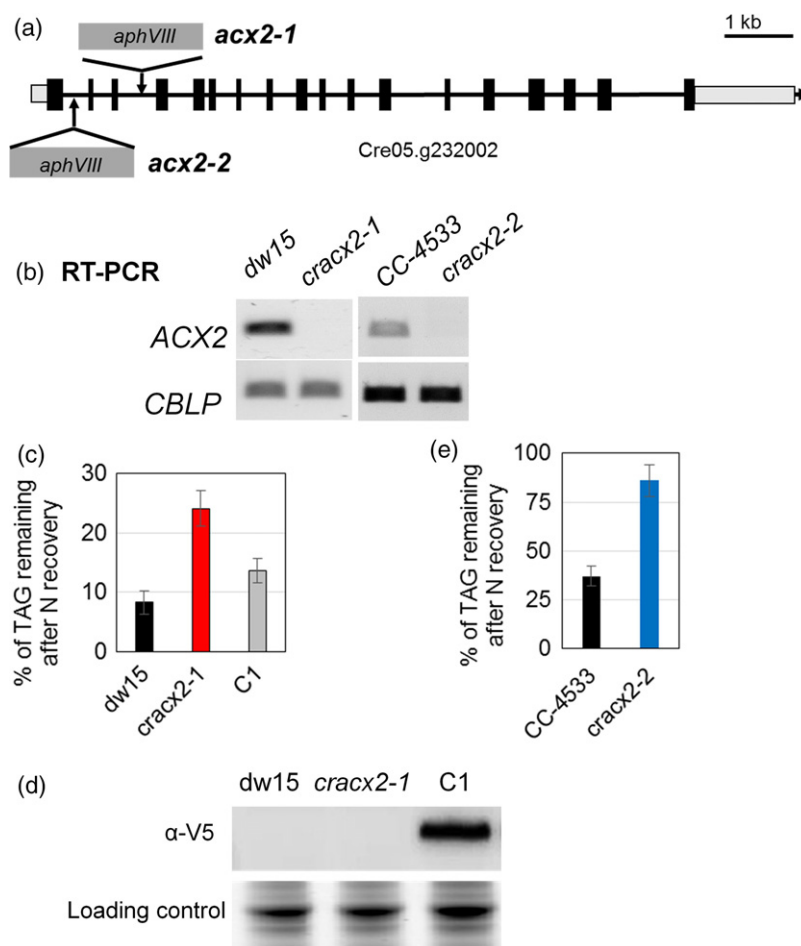
(c) Genetic complementation of *cracx2-1*. C1: a representative of the complemented strain.

(d) Immunoblot detection of the presence of *CrACX2* protein in the C1 line.

(e) Defect in oil remobilization in the mutant *cracx2-2* line.

(c,e) Cells were first starved of N for 3 days, then transferred to an N-containing medium to initiate oil remobilization. Cells were harvested for lipid analysis 24 h after the onset of oil degradation. The triacylglycerol (TAG) quantification data by TLC are representative of three biological replicates done at different times. Data are means of two biological replicates with two technical replicates each, and error bars indicate standard deviations.

(b) *CBLP* (Cre06.g278222) codes for a receptor of activated protein kinase C; (d) V5 is the recombinant protein fused at its N-terminus to the epitope V5. [Colour figure can be viewed at [wileyonlinelibrary.com](http://wileyonlinelibrary.com)].



supplemented MM medium and then cell density was monitored. We first evaluated the optimal oleic acid concentration for such a test in the WT. We observed that when the oleic acid concentration exceeds 0.8 mM cells started to bleach and eventually died (Figure S4), most likely due to the detergent property of FAs. An oleic acid concentration of 0.5 mM is optimal when added to a cell culture of  $2 \times 10^6$  cells  $\text{ml}^{-1}$ . We observed that 24 h after addition of 0.5 mM oleic acid, WT cells grew at a rate twice that of the mutant *cracx2-1* (Figure 3). Growth was arrested eventually, probably due to the exhaustion of oleic acid in the medium, because when additional oleic acid (0.5 mM) was then added to the same culture, regrowth was observed with the WT strain but not the *cracx2* mutant (Figure 3). We also observed a slower growth of the mutant compared with the WT in the control experiment (dotted lines in Figure 3), probably due to the fact that under strict carbon starvation,  $\beta$ -oxidation of FAs released from membrane lipids could provide another source of the carbon skeletons required for maintenance of growth. This test allows us to attribute the defect in oil utilization in the mutant to a block in FA  $\beta$ -oxidation. These data show that

functional FA  $\beta$ -oxidation is therefore essential in the redistribution of carbon skeletons occurring under strict carbon starvation in *C. reinhardtii*.

#### Turnover of FAs during diurnal growth is compromised in *cracx2* mutant cells

It has been observed in the marine unicellular stramenopile *Nannochloropsis oceanica* that total FA content varies during a day/night cycle, i.e. FAs accumulate during the day and degrade at night (Poliner *et al.*, 2015). This phenomenon was also observed here in *C. reinhardtii* when it was cultivated photoautotrophically under a day/night cycle (12 h/12 h) (Figure 4a). At the end of night period, the mutant retained >80% of total FAs accumulated at the end of day, in contrast to 60% in the WT (Figure 4b). A role of *CrACX2* in lipid turnover during the day/night cycle is consistent with high transcription of *CrACX2* during the night (Figure 4c, adapted from Zones *et al.*, 2015). Therefore, this study provides experimental evidence that functional FA  $\beta$ -oxidation is involved in lipid homeostasis during nutrient stress but also plays a role in lipid turnover following natural diurnal cycles.

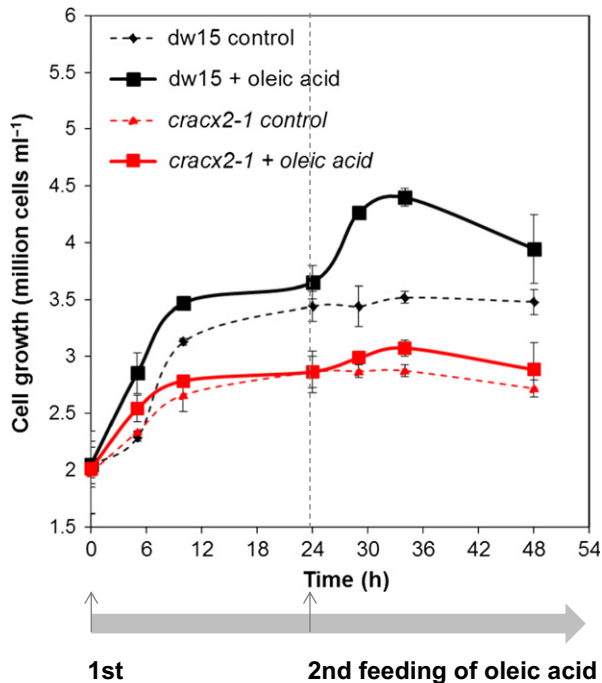


**Figure 3.** Oleic acid feeding test in *Chlamydomonas reinhardtii*. Cells were grown to mid log phase, then diluted to around 2 million cells ml<sup>-1</sup>. Either ethanol (as a control) or 0.5 mM oleic acid was added to each culture, and cells were then kept in the dark. The growth kinetics were followed up for a few days after the addition of oleic acid. Potential growth is seen as a result of oleic acid utilization. This is a representative figure for three independent biological replicates. Data are means of three technical replicates, and error bars indicate standard deviations. [Colour figure can be viewed at [wileyonlinelibrary.com](http://wileyonlinelibrary.com)].

### CrACX2 localizes to peroxisomes

No subcellular localization could be assigned for the CrACX2 using the PredAlgo prediction tool. This is not surprising, because in the design of the PredAlgo program, peroxisomes/microbodies are not included due to lack of known peroxisome protein sequences in algae (Tardif *et al.*, 2012). In order to determine in which compartment (peroxisomes or mitochondria) FA  $\beta$ -oxidation occurs in *Chlamydomonas*, we determined the subcellular localization of CrACX2, the first enzyme of the pathway. Sequence examination of the C-terminus or N-terminus of CrACX2 did not reveal obvious sequence similarity to either the peroxisome-targeting sequence (PTS1) [(S/C/A)(K/R/H)(L/M)] or the PTS2 [(R/K)(L/V/I)X<sub>5</sub>(H/Q)(L/A)] consensus sequence (Klein *et al.*, 2002; Hu *et al.*, 2012). This is different from the homolog of the two Arabidopsis proteins – AtACX2 contains a PTS2 sequence, whereas AtACX1 contains a typical PTS1 signal (Eastmond *et al.*, 2000) – but similar to ScPOX1 from *S. cerevisiae*, where no apparent PTS sequence is present but the protein is known to be imported into the peroxisomes through a novel non-PTS1 pathway (Klein *et al.*, 2002). The knockout mutant of

ScPOX1 cannot grow when oleic acid is present as the sole carbon source, thus demonstrating its essential role in the oxidative degradation of FAs in yeast peroxisomes (Dmochowska *et al.*, 1990).

To avoid a potential effect of protein mis-targeting or the occurrence of 'untypical' targeting sequences at its N- or C- terminus, we made two constructs, one with mCherry protein fused at the N-terminus and the other with mCherry fused at the C-terminus of CrACX2 (Figure S1b,c). CrMDH2 contains a typical PTS2 signal at its N-terminus and has previously been localized to peroxisomes in *C. reinhardtii* (Hayashi *et al.*, 2015); it was used here as a positive marker for peroxisomes. Either of the two constructs was co-transformed, independently, into the WT strain with the PTS2 sequence from CrMDH2 fused to GFP (Figure S1d). Protein fluorescence analyses using confocal microscopy demonstrated that the co-transformation of mCherry-CrACX2 and PTS2(MDH2)-GFP co-localize to peroxisomes in *C. reinhardtii* (Figure 5). Despite several attempts, no signals could be detected when mCherry was fused at the C-terminus of CrACX2 (CrACX2-mCherry). One of the reasons for this could be that the fusion of mCherry to the C-terminus of the CrACX2 could potentially interfere with correct protein targeting due to the likely presence of PTS1(-like) internal signal sequences close to the C-terminus (Kaur *et al.*, 2009).

### CrACX2 catalyzes the conversion of acyl-CoA to *trans*-2-enoyl-CoA and produces H<sub>2</sub>O<sub>2</sub>

Previous studies reported the occurrence of acyl-CoA oxidases in certain algal peroxisomes which do not produce H<sub>2</sub>O<sub>2</sub> but instead transfer the energy into water (Stabenau *et al.*, 1989). The absence of catalase in the peroxisomes of *Chlamydomonas* raised the question of whether H<sub>2</sub>O<sub>2</sub>-producing activities were present in its peroxisomes. To understand the molecular mechanism of this oxidative step in *Chlamydomonas*, we characterized the catalytic activity of CrACX2. A codon-optimized version of CrACX2 was cloned into an *E. coli* expression vector (Figure S5). In parallel, we also expressed AtACX2 in *E. coli* (Figure 6a). The AtACX2 protein is known to produce H<sub>2</sub>O<sub>2</sub> while oxidizing long chain fatty acyl-CoAs (Hooks *et al.*, 1999; Eastmond *et al.*, 2000). Purified recombinant CrACX2 protein catalyzed the conversion of acyl-CoAs to their respective *trans*-enoyl-CoA products, and produced H<sub>2</sub>O<sub>2</sub>. CrACX2 is more active toward long chain acyl-CoAs (C18:1-, C18:0-, C20:0-, C16:0-CoAs) than to medium chain acyl-CoA (C12:0-CoA) (Figure 6b). AtACX2 showed higher activity toward C18:1-CoA followed by C12:0-CoA, and had lower activity with C16:0-, C18:0- and C20:0-CoA (Figure 6b). The preference for mono-unsaturated CoAs over saturated CoA is consistent with a previous finding (Hooks *et al.*, 1999), whereas in our assay the Arabidopsis protein can also utilize C12:0-CoA.

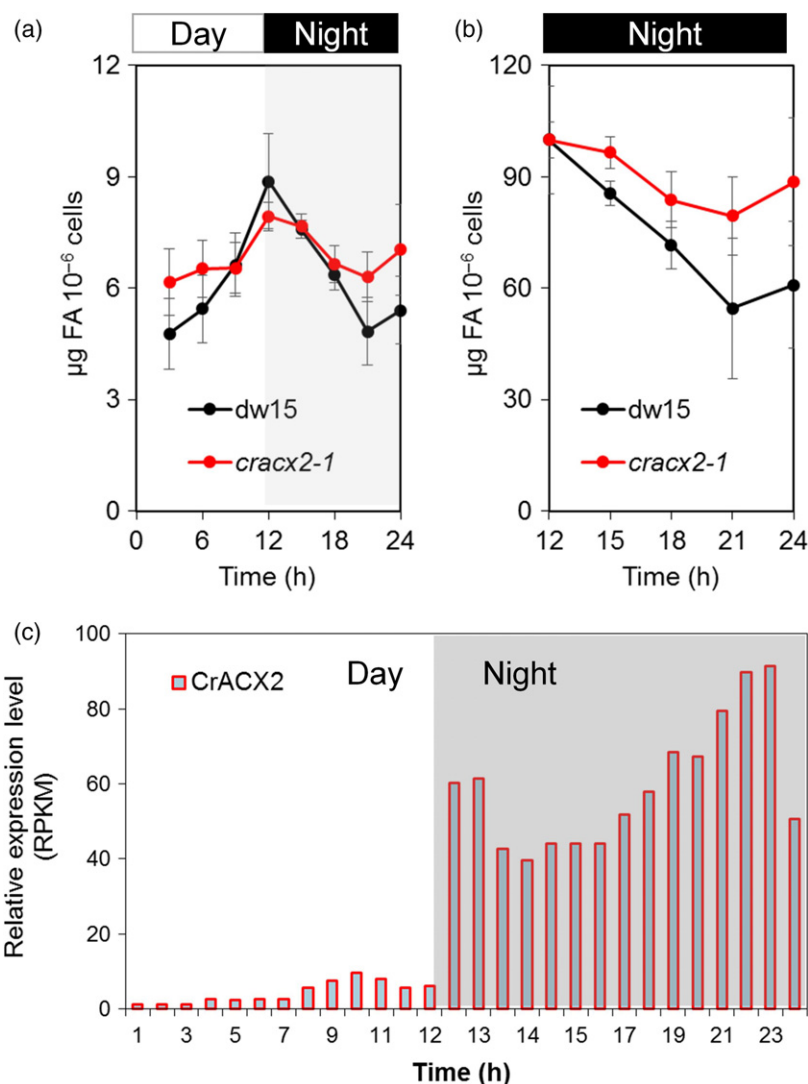
**Figure 4.** The *cracx2* mutant is impaired in fatty acid (FA) turnover during day/night cycles.

(a) Fluctuation of FA content during the day and night cycle in the wild type and the mutant.

(b) Percentage of FA retained during the night.

(c) Expression profile of *CrACX2* within a day/night (12 h/12 h) cycle (data are based on Zones *et al.*, 2015).

(a,b) Data are means of three biological replicates and with two technical replicate each. Error bars represent standard deviations. (c) RPKM stands for 'reads per kilobase per million mapped reads'. [Colour figure can be viewed at [wileyonlinelibrary.com](http://wileyonlinelibrary.com)].



Interestingly, the algal protein showed slightly broader activity toward different acyl-chain lengths than the plant protein (Figure 6b). This may at least partly explain why a strong phenotype can already be observed in the single mutant of *Chlamydomonas* (*cracx2*), whereas the single Arabidopsis mutant *atacx2* did not show any phenotype (Pinfield-Wells *et al.*, 2005). A defect in oil remobilization is only detectable in the Arabidopsis double mutant when both *AtACX1* and *AtACX2* are absent (Pinfield-Wells *et al.*, 2005). To conclude, ACX activity measurement showed that both the algal and plant proteins have wide substrate specificities toward a range of medium- to long-chain CoAs (Hooks *et al.*, 1999; Pinfield-Wells *et al.*, 2005), thus further supporting their essential role in FA  $\beta$ -oxidation. As previously demonstrated for the plant protein (*AtACX2*), *CrACX2* requires flavin adenine dinucleotide (FAD) as a cofactor (Figure 6). This is supported by the presence of signature amino acid sequences for FAD-binding (the GGGHGY motif)

and for long-chain acyl specificity (KWWI/PG/G/N) in *CrACX2*.

#### The *cracx2* mutant does not over-accumulate acyl-CoAs

We further asked if a block in the first step of the FA  $\beta$ -oxidation spiral resulted in over-accumulation of its precursors, i.e. free acyl-CoAs. Total acyl-CoAs were extracted and analyzed from the mutant as well as the WT by liquid chromatography coupled to mass spectrometry (LC-MS/MS) (see Methods S1). No significant difference in acyl-CoAs could be found between the WT and *cracx2-1* under any of the three conditions of optimal growth, N starvation and N resupply (Figure S6). Free FAs were not detected in the mutant either. This is consistent with the lack of growth defects in the mutant (Figure S7) because large amounts of free FAs are cytotoxic and can have negative impact on cell growth (Fan *et al.*, 2013a). This suggests that, in algae, there are tight metabolic regulations that coordinate cytosolic lipolysis with  $\beta$ -oxidation of FAs in the peroxisomes.

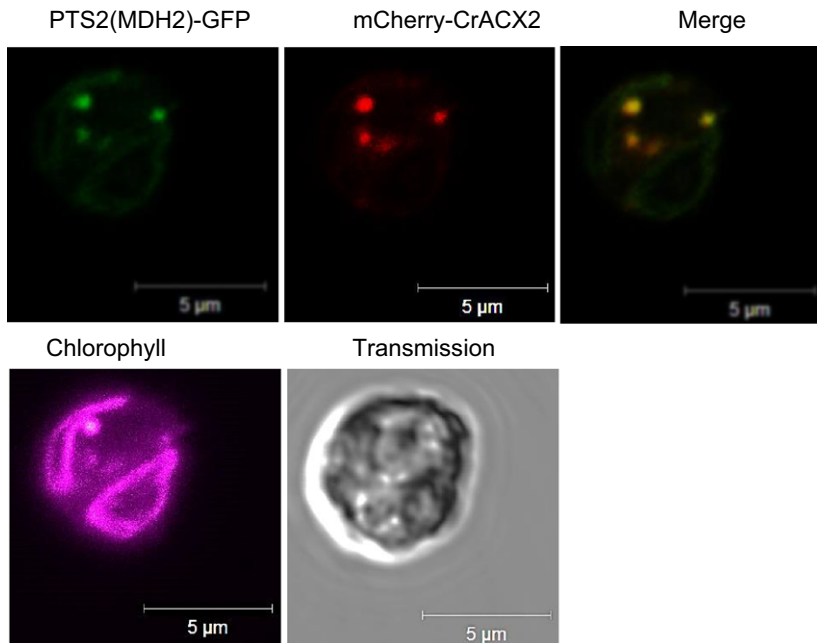


**Figure 5.** CrACX2 localizes to peroxisomes in *Chlamydomonas reinhardtii*.

Peroxisomal localization of mCherry-CrACX2 by confocal microscopy in a representative of transgenic lines expressing mCherry-tagged CrACX2. This line was created by co-transformation with a GFP-tagged PTS2 signal from the protein CrMDH2. Pseudo-colors are used. Chlorophyll autofluorescence is shown as magenta. GFP, green fluorescent protein; PTS, peroxisomal targeting signal; TRITC, tetramethylrhodamine isothiocyanate. [Colour figure can be viewed at [wileyonlinelibrary.com](http://wileyonlinelibrary.com)].

#### Cellular oil content is increased by 20% in *cracx2* mutants during N starvation

Quantitative RT-PCR analysis of the transcriptional expression level of *CrACX2* in the WT revealed that *CrACX2* expression is upregulated two-fold during the N recovery phase (Figure 7a), in accordance with its role in FA degradation. Moreover, we observed that it is repressed during N starvation, when active oil synthesis occurs. Therefore, we examined the changes in storage lipid content during the N starvation phase. As shown in Figure 7(b), a 20% increase in total TAGs was observed in the *cracx2-1* and *cracx2-2* mutants after 3 days of N starvation. Strikingly, this increase in TAG content is largely due to an increase in TAG52 molecular species (>55% increases) while there are no significant changes in TAG50 or TAG54 species (Figure 7c). The preferential increase in TAG52 lipid species suggests that during N starvation the cellular TAG pool is not metabolically inert but highly dynamic, conforming to the observations made previously either in germinating seeds of *Arabidopsis* FA  $\beta$ -oxidation mutants where TAG content and composition were altered due to simultaneous turnover and synthesis (Hernández *et al.*, 2012), or in actively growing vegetative tissues (Fan *et al.*, 2013b). During normal cultivation under standard mixotrophic condition, no significant differences were observed in terms of oil and polar lipid content and FA composition between WT and the mutant (Figure S8).

#### DISCUSSION

Increasing evidence suggests the importance of lipid catabolism in metabolically active cells, but no genes or

proteins involved in  $\beta$ -oxidation of FAs have so far been studied in detail in microalgae. Here, through a forward genetic screen in *C. reinhardtii*, we isolated the mutant *cracx2* defective in the first step of the core FA  $\beta$ -oxidation pathway. In-depth characterization of the mutant revealed that *Chlamydomonas*, an ancestral eukaryotic cell, harbors its FA degradation machinery in its peroxisomes, and defects in the normal functioning of this pathway increase cellular oil content under N starvation. Oil remobilization is severely, but not entirely, blocked in the *cracx2* mutant (Figures 1 and 2), which could be explained by the presence of at least four other ACX isozymes in *C. reinhardtii* (Table S1) (Merchant *et al.*, 2007; Li-Beisson *et al.*, 2015). These isozymes show at least 35% sequence identity to their closest *Arabidopsis* ACX proteins, where functional overlaps are well known because oil breakdown and seedling establishment are largely unaffected in any of the single mutants of *Arabidopsis* (Eastmond *et al.*, 2000; Graham and Eastmond, 2002; Pinfield-Wells *et al.*, 2005). Presumably, therefore, in the *cracx2* mutant the presence of the four other isozymes makes a partial contribution to the continued operation of the pathway.

#### $\beta$ -Oxidation of FAs occurs in *Chlamydomonas* peroxisomes

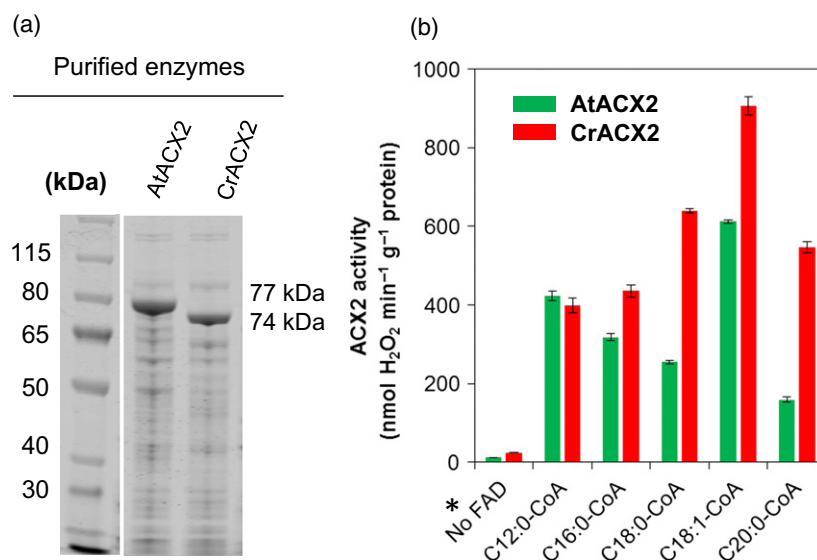
$\beta$ -Oxidation of FAs is one of the major lipid catabolic pathways, essential for converting fats to sugars in many organisms. Since its discovery over 100 years ago, the biochemistry and subcellular compartment harboring this pathway in microalgae has remained enigmatic. In this study, we demonstrate that *Chlamydomonas* houses the major reactions of FA  $\beta$ -oxidation in peroxisomes. Two



**Figure 6.** CrACX2 is a bona fide acyl-CoA oxidase. (a) Production of recombinant acyl-CoA oxidizing (ACX) protein in *Escherichia coli*.

(b) ACX enzymatic activities.

Data are means of four independent assays. Error bars represent standard deviations. \*Denotes the test including C18:1-CoA but with the absence of FAD. [Colour figure can be viewed at [wileyonlinelibrary.com](http://wileyonlinelibrary.com)].



lines of evidence support this claim: firstly the protein (CrACX2) catalyzing the initial step of the pathway is located in peroxisomes and not mitochondria; and secondly, biochemical analysis showed that CrACX2 is a bona fide oxidase, producing H<sub>2</sub>O<sub>2</sub>, rather than a dehydrogenase. All *Chlamydomonas* ACX proteins contain two acyl-CoA dehydrogenase domains and one acyl-CoA oxidase domain, a general feature of all known peroxisomal acyl-CoA oxidases (Eastmond *et al.*, 2000). Acyl-CoA oxidases and acyl-CoA dehydrogenases are two closely related enzyme families that are present in the peroxisome and mitochondria, respectively, and require FAD. They both catalyze the dehydrogenation of acyl-CoA to a *trans*-2-enoyl-CoA, but differ in the oxidative half of the reaction, i.e. acyl-CoA oxidase uses molecular oxygen to re-oxidize FADH<sub>2</sub>, thereby producing H<sub>2</sub>O<sub>2</sub>, whereas acyl-CoA dehydrogenase transfers the electrons to the mitochondrial respiratory chain and is thus coupled to ATP production (Kim and Miura, 2004; Poirier *et al.*, 2006). Protein structural studies have shed light on the similarities and differences in the functional mode of these two closely related proteins (Kim and Miura, 2004). No homologs of mammalian acyl-CoA dehydrogenase (Lea *et al.*, 2000) are encoded in the genome of *C. reinhardtii*. The protein showing the highest sequence similarity to mammalian acyl-CoA dehydrogenase in fact encodes a homolog of the Arabidopsis isovaleryl-coenzyme A dehydrogenase (AtIVD, At3g45300) known to be involved in breakdown of branched chain amino acids in the mitochondrion (Gu *et al.*, 2010). Based on this evidence, it is highly likely that *C. reinhardtii* employs a peroxisomal pathway for degradation of its oil reserves.

As well as the first reaction (i.e. ACX), the genome of *Chlamydomonas* also encodes all the other three enzymes catalyzing the subsequent steps of the FA  $\beta$ -oxidation spiral,

namely the two multifunctional proteins (enoyl-CoA hydratase, 3-hydroxyacyl-CoA dehydrogenase) and the ketoacyl-CoA thiolase (Li-Beisson *et al.*, 2015), and their expressions are also found to be higher in the dark than during the day (Zones *et al.*, 2015), suggesting a similar role in lipid turnover to that of CrACX2. Nevertheless, their exact contributions to degradation of FAs and their subcellular localization in algal cells remain to be validated experimentally.

The finding that *Chlamydomonas* employs a peroxisomal pathway to degrade FAs raised the question of why *Chlamydomonas* has adopted a peroxisomal pathway where energy is lost (through production of H<sub>2</sub>O<sub>2</sub> and its immediate conversion to H<sub>2</sub>O) in contrast to a mitochondrial pathway where FA degradation is tuned to energy production. One of the possible explanations is that *Chlamydomonas*, found in soil where large fluctuations in nutrient supply occur, opts for high metabolic fluxes at the cost of energy loss, rather than favoring energy conservation. This would be consistent with the extensive metabolic flexibility that *Chlamydomonas* displays, most likely as a result of adaptation to inhabit distinct environmental niches and to survive fluctuations in nutrient availability (Grossman *et al.*, 2007).

As well as acetyl-CoAs, the other end products of FA  $\beta$ -oxidation are H<sub>2</sub>O<sub>2</sub> and NADH. H<sub>2</sub>O<sub>2</sub>-producing activity is a key feature and is behind the naming this organelle a 'peroxisome' (Kaur *et al.*, 2009). H<sub>2</sub>O<sub>2</sub> is highly oxidative, and potentially damaging to cellular components including DNA, proteins and lipids. Due to the absence of catalase in the peroxisomes of *Chlamydomonas* (Kato *et al.*, 1997), other reactive oxygen species (ROS)-detoxifying enzymes in the peroxisome must function to quench H<sub>2</sub>O<sub>2</sub> produced during the period of active oil degradation. An alternative is the ascorbate peroxidase (APX)/monodehydroascorbate reductase (MDAR) electron transfer system. Indeed disruption of the MDAR system in Arabidopsis results in

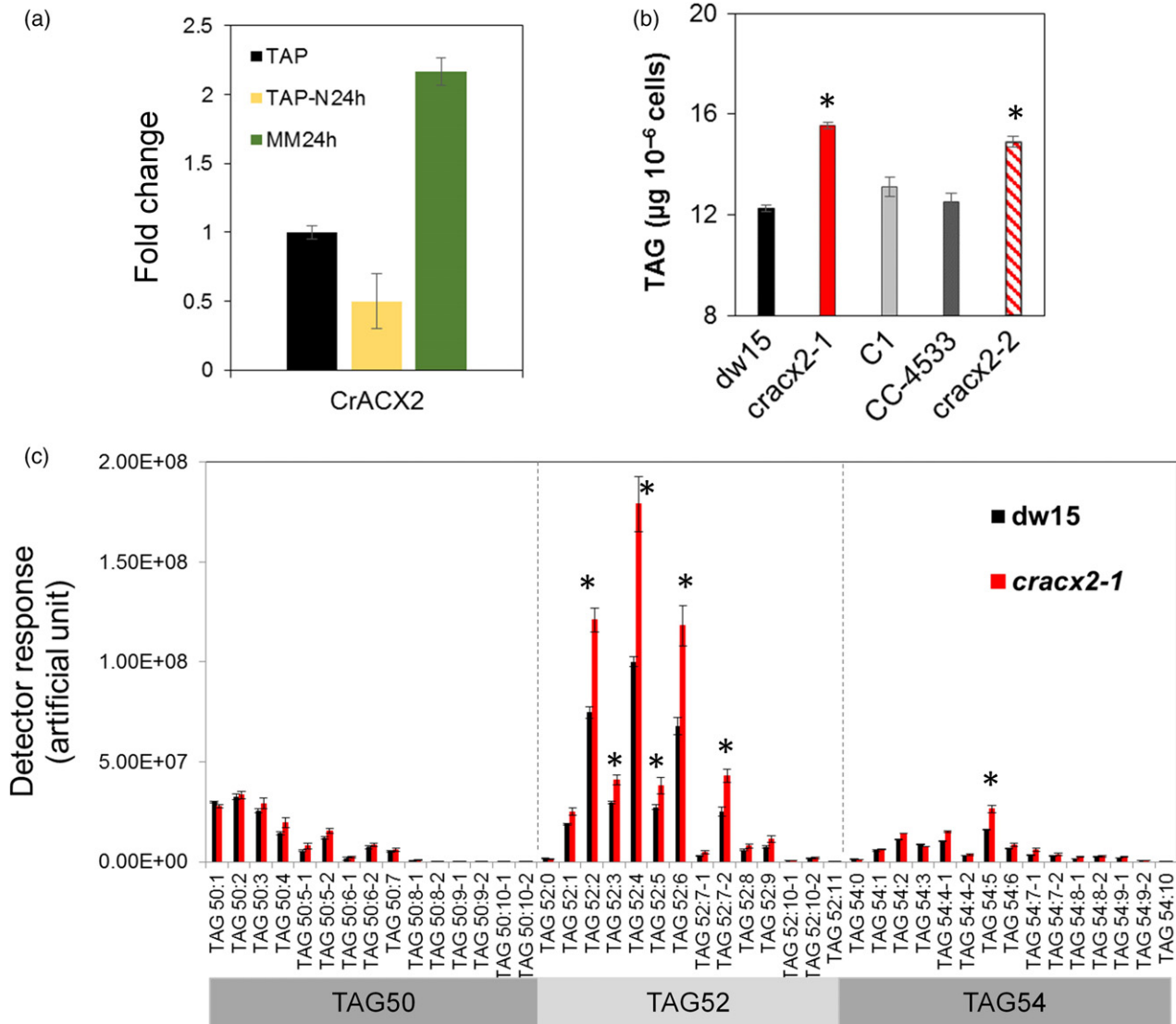


**Figure 7.** Oil content analysis of cells starved of nitrogen.

(a) Quantitative RT-PCR analysis of transcriptional responses of *CrACX2* to differing N status in the wild type. Data are fold changes compared with the expression level determined for optimally grown cells (in acetate containing medium, TAP). The housekeeping gene used is *RACK1*. Data are means of three biological replicates, and with two technical replicates each. This is a representative of three independent experiments.

(b) Comparison of triacylglycerol (TAG) content.

(c) Analysis of molecular species of TAGs by LC-MS/MS. Data are means of three biological replicates with two technical replicates each; error bars represent standard deviations. Detector response has been normalized based on cell numbers. \*Significant difference between strains. Statistical analysis was carried out using the Student's *t*-test ( $P < 0.05$ ). [Colour figure can be viewed at [wileyonlinelibrary.com](http://wileyonlinelibrary.com)].

impaired oil catabolism through inhibition of the sugar dependent-1 (SDP1) lipase activity by escaped  $\text{H}_2\text{O}_2$  (Eastmond, 2007). This APX/MDAR membrane-bound system has been shown to possess a much higher affinity than catalase for  $\text{H}_2\text{O}_2$  (Lisenbee *et al.*, 2003, 2005). Another possible route includes hydroxypyruvate reductase (HPR) and also a peroxisomal NADH transporter. Deficiencies in these proteins have resulted in plants impaired in oil breakdown (Pracharoenwattana *et al.*, 2010; Bernhardt *et al.*, 2012). Enzymes homologous to known Arabidopsis

proteins are encoded in the genome of *Chlamydomonas* (Merchant *et al.*, 2007). The contribution of these proteins to lipid catabolism in algal peroxisomes needs to be tested in the future once corresponding mutants are available.

#### Physiological roles of FA $\beta$ -oxidation in *Chlamydomonas*

The isolation of the *cracx2* mutants in this study provided us with a means not only to probe the role of FA  $\beta$ -oxidation in oxidative degradation of lipids, but also to experimentally test the physiological functions of peroxisomes in

*C. reinhardtii*. The increase in oil content in the *cracx2* mutants under N starvation supports the idea that FA turnover is ubiquitous, occurs simultaneously with active oil synthesis in green algae and also plays a role in carbon management during day/night cycles.

Peroxisomal  $\beta$ -oxidation in fungi is primarily devoted to the degradation of extracellular FAs supplied in the diet for the subsequent use of acetyl-CoA as a carbon source for growth. In this study, we showed that when supplied at low concentrations, and in the absence of other carbon sources (during carbon starvation condition), *Chlamydomonas* can convert FAs to sugars to power growth, whereas mutant defective in the normal function of the  $\beta$ -oxidation cycle cannot. This might not be a major catabolic reaction, but it is significant enough to sustain growth under strict carbon starvation, which might be critical for survival under extreme environmental conditions.

In plant tissues, the most studied physiological function has been the utilization of internal neutral lipids in storage tissues (e.g. seeds); this allows cells to convert stored TAGs to sugars. Intensive research in the last 10 years has also started to uncover the essential functions of FA  $\beta$ -oxidation in other aspects of growth and development, especially in active photosynthetic cells, including their vital role under prolonged carbohydrate starvation in extended darkness (Kunz *et al.*, 2009), namely the synthesis of FA-based signaling molecules, degradation of branched chain amino acids and their roles in flower development (Gerhardt, 1992; Hu *et al.*, 2012).

To prevent lipotoxicity, cells have developed sophisticated mechanisms to coordinate the synthesis and metabolism of their FAs. To avoid a large flux of acyl-chains entering the cytoplasm, the sequestration of acyl-chains into TAGs stored in LDs has been shown to be an effective way to protect cells in plant vegetative tissues (Fan *et al.*, 2014), as well as in mammalian cells (Rambold *et al.*, 2015), from lipotoxic damage. This study suggests that TAGs could also serve as a temporary reservoir for acyl-groups in the green alga *C. reinhardtii*. This is evidenced by the fact that during N starvation, massive degradation of membrane lipids occurs (Siaut *et al.*, 2011) and the extra fluxes of acyl-chains were therefore sequestered in TAGs. The amount of TAGs produced is even higher in the mutant cells where FA  $\beta$ -oxidation has been shut down.

### Peroxisome biology and algal biotechnology

Research on algal peroxisomes has been limited compared with that on other organelles due to their elusive nature and associated technical challenges. Only fairly recently have peroxisomes been visualized and shown to occur in *Chlamydomonas* (Shinozaki *et al.*, 2005, 2009; Hayashi and Shinozaki, 2012; Hayashi *et al.*, 2015). Since then, microscopy and fluorescence protein tagging studies have shown that homologs of the known proteins of the

glyoxylate cycle, apart from isocitrate lyase (ICL), are located in the peroxisomes of *C. reinhardtii* (Lauersen *et al.*, 2016). Among the putative glyoxylate enzymes, only ICL, found to be located in the cytosol, has been shown to be essential for a functional glyoxylate cycle because the null mutant *icl* cannot grow in the dark when only acetate is available as a carbon source (Plancke *et al.*, 2014; Lauersen *et al.*, 2016). Thus, there had previously been no functional demonstration of the involvement of the peroxisome-based glyoxylate cycle proteins in acetate metabolism and little was known about metabolism occurring in the peroxisomes of *C. reinhardtii*.

This study provides experimental data to demonstrate the active involvement of peroxisomes in subcellular metabolism in *C. reinhardtii* – highlighting its central place as an ‘organelle at the crossroads’ in green microalgae. It would be interesting to determine in future studies if conversion of fats to sugars in *Chlamydomonas* requires the coupling of FA  $\beta$ -oxidation to the peroxisomal glyoxylate cycle as occurs in plants (Pracharoenwattana *et al.*, 2005), or if it can function independently as is the case in *S. cerevisiae*, due to the presence of a carnitine shuttle (Vanroermund *et al.*, 1995; Graham and Eastmond, 2002).

Shutting down FA  $\beta$ -oxidation led to augmented levels of TAGs, further demonstrating the dynamic nature of lipid turnover in *Chlamydomonas*. Impairment in lipid catabolism has previously been shown to increase lipid content (Slocombe *et al.*, 2009; Fan *et al.*, 2013b; Trentacoste *et al.*, 2013), but this study provides the first such example for green microalgae. Considering the increasing interest in developing algae as a platform for the production of biomaterials, and the central place the peroxisome occupies in cellular metabolism, the capacity to manipulate metabolism in peroxisomes seems essential. For example, one of the often neglected functions of FA  $\beta$ -oxidation is its ‘house-keeping’ function during normal development, i.e. preventing the integration of ‘exotic’ FAs into membranes. This house-keeping role is particularly amplified in transgenic plants synthesizing ‘unusual’ FAs where FA  $\beta$ -oxidation is enhanced (Jaworski and Cahoon, 2003; Moire *et al.*, 2004). Thus, knowledge gained through this study should be useful not only for production of biodiesel and other functional FAs in microalgae, but will also have implications for algal fitness and biomass productivity.

### EXPERIMENTAL PROCEDURES

#### *Chlamydomonas reinhardtii* strains and culture conditions

*Chlamydomonas reinhardtii* strain *dw15.1* (*nit1-305 cw15; mt<sup>+</sup>*) was used to generate the mutant library (Cagnon *et al.*, 2013). Independent paromomycin-resistant ( $10 \mu\text{g ml}^{-1}$ ) clones were screened for oil content by flow cytometry after Nile Red staining. *Chlamydomonas reinhardtii* can be cultivated photoautotrophically (MM medium supplied with 2% CO<sub>2</sub> in air) (Cagnon *et al.*, 2013) or mixotrophically in TAP medium (Harris, 2001). For all

cultures, cells were cultivated in an incubator (Infors, <http://www.infors-ht.co.uk/en>) (25°C, 100 rpm shaking, and illuminated at 100  $\mu\text{mol photons m}^{-2} \text{sec}^{-1}$ ). To induce N starvation, exponentially grown cells were centrifuged at 600 *g* for 5 min, washed twice in N-free medium and finally resuspended in TAP-N or MM-N. Cell concentrations were determined using a Multisizer 3 Coulter counter (Beckman Coulter, <https://www.beckmancoulter.com/>). Exponentially grown cells were harvested for all analyses.

The strain LMJ.SG0182.014586 harboring an insertion in the gene encoding CrACX2 was ordered, together with its parental line CC-4533, from the Martin Jonikas collection (Li *et al.*, 2016; <https://www.chlamylibrary.org/>). Null expression in the CrACX2 gene was verified by RT-PCR using the primers ACX-F2 and ACX-R2, and control PCR was done via amplification of the CBLP gene using primers CBLP-F2 and CBLP-R2. The sequences for these and all the other primers used are given in Table S2.

### Identification of the insertion site by RESDA-PCR

The genomic region(s) flanking the inserted DNA (*AphVIII*) were characterized by RESDA-PCR (González-Ballester *et al.*, 2005), which allows amplification from primers with a known sequence into adjacent regions using degenerate primers containing restriction enzyme site sequences that are frequent in the *Chlamydomonas* genome (*AluI*, *PstI*, *SacI* or *TaqI*). Specific primers (RB1 and RB4) at the 3' regions of *AphVIII*, and the degenerate primers (DegPstI and DegTaqI) and specific primer (Q0) targeted to degenerate primers, were used for RESDA-PCR to amplify the DNA from the possible regions affected. The amplified PCR product (around 0.8–1.0 kb) was sequenced. Blast searches of the amplified flanking sequences against the genome of *C. reinhardtii* (v5.5) (Merchant *et al.*, 2007) located at Phytozome (v10.3) identified the insertion site.

### Quantification of gene expression by real-time PCR

Quantification of CrACX2 expression by real-time PCR (qRT-PCR) was performed on the LightCycler 480 System (Roche, <http://www.roche.com/>) using 2.5  $\mu\text{l}$  of SYBR Premix Ex Taq II (Takara, [www.clontech.com](http://www.clontech.com)) in a final volume of 5.0  $\mu\text{l}$  with 2.0  $\mu\text{l}$  first cDNA strand synthesized as described above and 0.5  $\mu\text{l}$  of 3 pmol of each primer. The specific primer set (qACX2 F and qACX2 R) was used to amplify a 135-bp CrACX2 cDNA fragment. The amplification conditions were as follows: 95°C for 10 min, followed by 45 cycles of 10 sec at 95°C, 15 sec at 60°C and 10 sec at 72°C. The specificity of PCR amplifications was checked by a melting curve program (95°C for 5 sec, 65°C for 10 sec, continuous acquisition at 95°C and cooling at 40°C for 30 sec) and analyzed by electrophoresis on a 2.0% agarose gel. The data were normalized as relative values with respect to the housekeeping gene *RACK1* (*Cre06.g278222*) (Nguyen *et al.*, 2013).

### RNA extraction, reverse transcription (RT)-PCR, gene cloning and *Chlamydomonas* transformation

Total RNA was isolated as previously described (Nguyen *et al.*, 2013). Purified total RNA was treated with DNase I (Ambion, Invitrogen, [www.thermofisher.com](http://www.thermofisher.com)) to remove the contaminated residual genomic DNA, and was then purified with Nucleospin RNA Clean Up (Macherey Nagel, <http://www.mn-net.com/>). First-strand cDNA was synthesized from total RNA (1  $\mu\text{g}$ ) with the SuperScript VILO cDNA Synthesis Kit (Life Technologies, [www.thermofisher.com](http://www.thermofisher.com)). For RT-PCR, a fragment of the cDNA coding region of CrACX2 was amplified using the gene-specific primers ACX-F1 and ACX-R1. CBLP (*Cre06.g278222*) was amplified using primers

CBLP-F1 and CBLP-R1, and was used as a housekeeping gene for normalization (Kong *et al.*, 2015).

The cDNA sequences of CrACX2 (*Cre05.g232002.t2.1*) was amplified using the gene-specific primers *KpnI*-ACX2-F2 and *XbaI*-ACX2-R2. The PCR reaction was carried out using high-fidelity KOD Hot Start DNA Polymerase (Merck Millipore, <http://www.merckmillipore.com/>). The amplified DNA fragment was cloned as a *KpnI*-*XbaI* fragment into the pChlamy4 vector (Life Technologies) which contains the *ble* gene conferring zeocin resistance (Stevens *et al.*, 1996; Kong *et al.*, 2015), generating the plasmid pChlamy4-cACX2. The target gene was cloned in-frame with a V5 tag at its 3' end, allowing screening of complemented lines by anti-V5 (GKPIPPLGLDST) antibodies.

pChlamy4-cACX2 was integrated into the *cracx2-1* genome by electroporation (Shimogawara *et al.*, 1998). Briefly, exponentially grown cells (about 20 million) were harvested by centrifugation and suspended in 250  $\mu\text{l}$  of TAP medium supplemented with 40 mM sucrose. Electroporation was performed by applying an electric pulse of 0.7 kV at a capacitance of 50  $\mu\text{F}$  (GENE PULSER, Bio-Rad, <http://www.bio-rad.com/>) to cells mixed with 0.3  $\mu\text{g}$  of *SspI*-linearized plasmids. The transgenic strains were selected directly on TAP agar plates containing zeocin (25 mg L<sup>-1</sup>), and the plates were incubated under continuous light (50  $\mu\text{mol photons m}^{-2} \text{sec}^{-1}$ ) at 25°C. Colonies resistant to zeocin were visible after around 7 days. The presence of the cassette in the transformants in some selected strains was determined by PCR with amplification by the primers ACXcloneF and RBcS2 R.

### Oleic acid feeding test

Oleic acid (Sigma-Aldrich, <http://www.sigmaaldrich.com/>) at a final concentration of 0.5 mM from a 1 M stock solution in ethanol was added to pre-cultures grown photoautotrophically. The same volume of ethanol was added to the controls. The capacity to use oleic acid as a carbon source was determined by cell growth in the dark at 25°C.

### Protein extraction and immunoblot analysis

Total proteins were extracted from *Chlamydomonas* cells following the method described in Nguyen *et al.* (2013). Protein concentrations were determined spectrophotometrically at 280 nm using a BCA protein assay kit (Bio-Rad). For immunoblot, approximately 15  $\mu\text{g}$  of proteins were separated on 12% SDS-PAGE, transferred to a nitrocellulose membrane (Sigma-Aldrich) using the semidry transfer technique and immunoblotted with specific polyclonal rabbit anti-V5 primary antibodies (1/5000) (eBioscience, <https://www.ebioscience.com/>) for detecting the V5-tagged proteins. The chemiluminescent substrate CDP-Star (Roche) was used to detect immunoreactive proteins by utilizing secondary antibodies conjugated to the anti-rabbit IgG-fluorescein isothiocyanate (FITC) (1/20 000). Blots were imaged using the G:BOX Chemi XRQ system (Syngene, <http://www.syngene.com/>).

### Lipid extraction and analyses

Freshly grown cells were harvested and either quenched immediately in boiling isopropanol or kept frozen in liquid nitrogen. A hot isopropanol method was used to extract the total lipids (Légeret *et al.*, 2016). Extracted lipids were dried under a stream of N<sub>2</sub> and then dissolved either in a mixture of chloroform:methanol (2:1 by volume) for TLC or in a solvent mixture of acetonitrile:isopropanol:10 mM ammonium acetate (65:30:5 by volume) for LC-MS/MS. Depending on the analysis required, lipid standards TAG51:0(17:0/17:0) and PtdEtn34:0 (17:0/17:0) (Sigma-

Aldrich), were added just before the solvent extraction step. Detailed TLC procedures and quantifications have been described in Légeret *et al.* (2016) and Siaux *et al.* (2011).

### Nile red staining of LDs and confocal microscopy

Lipid droplets in live cells were first stained with a Nile red solution ( $1 \mu\text{g ml}^{-1}$ ), kept for 10 min in the dark and then imaged with a confocal laser scanning microscope (TCS SP2, Leica, <http://www.leica-microsystems.com/>). A  $63\times$  oil immersion objective was used throughout all the imaging work. Cells were excited using a laser excitation line at 488 nm, emission for the Nile red signal was collected between 554 and 599 nm and the chlorophyll autofluorescence signal was collected between 650 and 714 nm. Pseudo colors were obtained for all images using ZEN (Carl Zeiss, <http://www.zeiss.com/>) software.

### Subcellular localization of CrACX2

**Constructs for protein subcellular localization.** CrACX2 was cloned in frame to the C-terminus of an mCherry cassette. The full-length CrACX2 open reading frame (ORF) was amplified by *KpnI*-ACXf and *XbaI*-ACXr primers, and inserted into the pChlamy3 plasmid as a *KpnI/XbaI* fragment, resulting in the recombinant plasmid pChlamy3-ACX2. The mCherry ORF was amplified by InFUMCherryF and InFUMCherryR from the pBR9 mCherry Cr plasmid (Rasala *et al.*, 2013). The mCherry ORF was fused in frame to the N-terminus or C-terminus of CrACX2 to construct the recombinant plasmid mCherry-ACX2, or ACX2-mCherry, by an In-Fusion<sup>®</sup> HD cloning kit (Clontech, <http://www.clontech.com/>). The known PTS2 (MADPLNRIQKIASHLDPKPRKFKVA) for CrMDH2 was cloned using the primers *NdeI*-PTSf and *XhoI*-PTSr and integrated into pBR9 GFP plasmid as a *NdeI/XhoI* fragment (Rasala *et al.*, 2013). The *AphVIII* gene was amplified from the pSI103 plasmid (Sizova *et al.*, 2001) by *Aph8*-infusF and *Aph8*-infusR primers and cloned into PTS2(MDH2)-GFP plasmid. The mCherry-ACX2, or ACX2-mCherry, and PTS2(MDH2)-GFP plasmids were co-transformed to the *dw15* strain, and the double transformants were selected on agar plates containing both hygromycin B ( $15 \mu\text{g ml}^{-1}$ ) and paromomycin ( $10 \mu\text{g ml}^{-1}$ ).

**Fluorescence microscopy.** For live cell fluorescence microscopy, representative clones of co-transformants were grown in TAP medium to log phase. Images were captured on a confocal microscope (TCS SP2; Leica). The cells were excited with a 488-nm laser line. The following filters were used: for mCherry, excitation at 561 nm and emission 610–630 nm; for GFP, excitation at 458 nm and emission at 500–530 nm; and for chlorophyll autofluorescence, excitation at 645 nm and emission at 685–720 nm.

### Protein expression in *E. coli* and *in vitro* assays for ACX activity

The codon-optimized CrACX2 cDNA was synthesized by GenArts (Invitrogen). It was then amplified using Lic07eCrACXf and Lic07e-CrACXr primers. The fragment was cloned into plasmid Lic07 with an In-Fusion<sup>®</sup> HD cloning kit (Clontech) and then transformed into *E. coli* strain BL21. The AtACX2 was cloned using the primers AtACX2-F and AtACX2-R. For protein expression, pre-cultures were grown in 50 ml of standard Luria broth overnight at 37°C. A small aliquot (10 ml) was added to 500 ml of fresh Terrific Broth and the cells grown at 37°C to an optical density ( $\text{OD}_{600 \text{ nm}}$ ) of approximately 1.0. Isopropyl  $\beta$ -D-1-thiogalactopyranoside (IPTG) was added to a final concentration of 0.5 mM and cultures were incubated overnight at 18°C. The cells were harvested by

centrifugation at 4000 *g* at 22°C for 30 min and re-suspended in 25 ml of lysis buffer [50 mM 2-amino-2-(hydroxymethyl)-1,3-propanediol (TRIS) pH 8.0, 500 mM NaCl, 10 mM imidazole, 10% glycerol,  $10 \mu\text{g ml}^{-1}$  DNase, 20 mM  $\text{MgSO}_4$  and  $0.25 \text{ mg ml}^{-1}$  lysozyme]. The cells were lysed by sonication three times with a 10-sec interval cycle. The cell debris was centrifuged at 21 000 *g* for 10 min in a microcentrifuge and the protein purified with a His GraviTrap kit (GE Healthcare, <http://www3.gehealthcare.com/>) according to the manufacturer's instructions.

The eluate was used for determining ACX activity as described previously (Hryb and Hogg, 1979; Hooks *et al.*, 1999). Briefly, the reaction mixture (50  $\mu\text{M}$  an acyl-CoA substrate, 50  $\mu\text{M}$  FAD, 5  $\mu\text{g}$  of purified enzyme and 175 mM TRIS pH 7.4) were incubated at 30°C for 30 min. The acyl-CoA substrates tested are lauroyl-CoA (C12:0-CoA), palmitoyl-CoA (C16:0-CoA), stearoyl-CoA (C18:0-CoA), oleoyl-CoA (C18:1-CoA) and arachidoyl-CoA (C20:0-CoA). Except for the C20:0-CoA (from Avantis Polar, <https://avantilipids.com/>), all other acyl-CoAs were ordered from Sigma-Aldrich. Stock solutions were made for each acyl-CoA by dissolving it into a 100 mM 2-(*N*-morpholino)ethanesulfonic acid (MES) buffer adjusted to pH 5.8 (for long-term storage); for reactions, pH was adjusted to 7.4. The final concentration of the acyl-CoA in the stock solution was determined by measuring the absorbance at 260 nm ( $E_{260} = 16.4$  at pH 7.4). For  $\text{H}_2\text{O}_2$  measurement, an Amplex<sup>®</sup> red hydrogen peroxide/peroxidase assay kit (Invitrogen) was used according to the manufacturer's instructions, and a Xenius XC spectrofluorometer (SAFAS, <http://www.safas.com/>) was used to measure the fluorescence emission at 580 nm (excitation at 540 nm) during the linear kinetic range.

### ACCESSION NUMBERS

Sequence data presented in this article can be found for *C. reinhardtii* genes in Phytozome ([https://phytozome.jgi.doe.gov/pz/portal.html#!info?alias=Org\\_Creinhardtii](https://phytozome.jgi.doe.gov/pz/portal.html#!info?alias=Org_Creinhardtii)) with gene identifications as: CrACX2 (*Cre05.g232002.t2.1*), CrMDH2 (*Cre10.g423250*) and RACK1 (*Cre06.g278222*). The Arabidopsis AtACX2 protein (At5g65110) and AtACX1 (At4g16760) can be found at The Arabidopsis Information Resource (<https://www.arabidopsis.org/>).

### ACKNOWLEDGEMENTS

We thank Pascaline Auroy, Cyril Aselmeyer, Audrey Beynel and Marie-Christine Thibaud for excellent technical assistance. We also thank Dr Peter Eastmond for useful discussions on acyl-CoA oxidase activity assays. Yuanxue Liang acknowledges the China Scholarship Council (CSC) for a Postgraduate Award. Work in the authors' laboratory is supported by A\*MIDEX project and ANR MUsCA. Support for the microscopy equipment was provided by the Région Provence Alpes Côte d'Azur, the Conseil Général des Bouches-du-Rhône, the French Ministry of Research, the CNRS and the CEA. We thank the European Union Regional Developing Fund (ERDF), the Région Provence Alpes Côte d'Azur, the French Ministry of Research and the CEA for funding the HélioBiotec platform. The authors declare no conflicts of interest.

### AUTHOR CONTRIBUTIONS

FK, FB, GP and YL-B designed the research; FK, YL, BL, AB-A, SB and RPH performed experiments and analyzed data; JAN contributed new analytical tools; and FK, FB, GP and YL-B wrote the paper.

## SUPPORTING INFORMATION

Additional Supporting Information may be found in the online version of this article.

**Figure S1.** Constructs used for genetic complementation and protein subcellular localization studies.

**Figure S2.** Examples of some of the screening results for genetic complementation.

**Figure S3.** Dynamic changes in absolute triacylglycerol content in the two mutant alleles and their corresponding wild-type strain.

**Figure S4.** Oleic acid feeding test.

**Figure S5.** Constructs for expression in *Escherichia coli*.

**Figure S6.** Quantification of acyl-CoAs by LC-MS/MS.

**Figure S7.** Growth kinetics under mixotrophic and photoautotrophic conditions.

**Figure S8.** Fatty acid and lipid composition of the wild type and mutant cells during optimal growth.

**Table S1.** The family of acyl-CoA oxidases in *Chlamydomonas reinhardtii*.

**Table S2.** All primer sequences used in this study.

**Methods S1.** Acyl-CoA profiling.

## REFERENCES

- Bernhardt, K., Wilkinson, S., Weber, A.P.M. and Linka, N. (2012) A peroxisomal carrier delivers NAD<sup>+</sup> and contributes to optimal fatty acid degradation during storage oil mobilization. *Plant J.* **69**, 1–13.
- Cagnon, C., Mirabella, B., Nguyen, H.M., Beyly-Adriano, A., Bouvet, S., Cuine, S., Beisson, F., Peltier, G. and Li-Beisson, Y. (2013) Development of a forward genetic screen to isolate oil mutants in the green microalga *Chlamydomonas reinhardtii*. *Biotechnol. Biofuels*, **6**, 178.
- Daum, G., Wagner, A., Czabany, T. and Athenstaedt, K. (2007) Dynamics of neutral lipid storage and mobilization in yeast. *Biochimie*, **89**, 243–248.
- Dmochowska, A., Dignard, D., Maleszka, R. and Thomas, D.Y. (1990) Structure and transcriptional control of the *Saccharomyces cerevisiae* POX1 gene encoding acylcoenzyme A oxidase. *Gene*, **88**, 247–252.
- Eastmond, P.J. (2007) Monodehydroascorbate reductase 4 is required for seed storage oil hydrolysis and postgerminative growth in *Arabidopsis*. *Plant Cell*, **19**, 1376–1387.
- Eastmond, P.J., Hooks, M. and Graham, I.A. (2000) The *Arabidopsis* acyl-CoA oxidase gene family. *Biochem. Soc. Trans.* **28**, 755–757.
- Eaton, S. (2002) Control of mitochondrial beta-oxidation flux. *Prog. Lipid Res.* **41**, 197–239.
- Fan, J.L., Andre, C. and Xu, C.C. (2011) A chloroplast pathway for the de novo biosynthesis of triacylglycerol in *Chlamydomonas reinhardtii*. *FEBS Lett.* **585**, 1985–1991.
- Fan, J., Yan, C. and Xu, C. (2013a) Phospholipid:diacylglycerol acyltransferase-mediated triacylglycerol biosynthesis is crucial for protection against fatty acid-induced cell death in growing tissues of *Arabidopsis*. *Plant J.* **76**, 930–942.
- Fan, J., Yan, C., Zhang, X. and Xu, C. (2013b) Dual role for phospholipid:diacylglycerol acyltransferase: enhancing fatty acid synthesis and diverting fatty acids from membrane lipids to triacylglycerol in *Arabidopsis* leaves. *Plant Cell*, **25**, 3506–3518.
- Fan, J., Yan, C., Roston, R., Shanklin, J. and Xu, C. (2014) *Arabidopsis* lipins, PDAT1 acyltransferase, and SDP1 triacylglycerol lipase synergistically direct fatty acids toward beta-oxidation, thereby maintaining membrane lipid homeostasis. *Plant Cell*, **26**, 4119–4134.
- Gasser, B., Prielhofer, R., Marx, H., Maurer, M., Nocon, J., Steiger, M., Puxbaum, V., Sauer, M. and Mattanovich, D. (2013) *Pichia pastoris*: protein production host and model organism for biomedical research. *Future Microbiol.* **8**, 191–208.
- Gerhardt, B. (1992) Fatty acid degradation in plants. *Prog. Lipid Res.* **31**, 417–446.
- Gonzalez-Ballester, D., Pootakham, W., Mus, F. et al. (2011) Reverse genetics in *Chlamydomonas*: a platform for isolating insertional mutants. *Plant Methods*, **7**, 24–37.
- González-Ballester, D., de Montaigu, A., Higuera, J.J., Galván, A. and Fernández, E. (2005) Functional genomics of the regulation of the nitrate assimilation pathway in *Chlamydomonas*. *Plant Physiol.* **137**, 522–533.
- Graham, I.A. (2008) Seed storage oil mobilization. *Annu. Rev. Plant Biol.* **59**, 115–142.
- Graham, I.A. and Eastmond, P.J. (2002) Pathways of straight and branched chain fatty acid catabolism in higher plants. *Prog. Lipid Res.* **41**, 156–181.
- Grossman, A., Croft, M., Gladyshev, V., Merchant, S., Posewitz, M., Prochnik, S. and Spalding, M. (2007) Novel metabolism in *Chlamydomonas* through the lens of genomics. *Curr. Opin. Plant Biol.* **10**, 190–198.
- Gu, L., Jones, A.D. and Last, R.L. (2010) Broad connections in the *Arabidopsis* seed metabolic network revealed by metabolite profiling of an amino acid catabolism mutant. *Plant J.* **61**, 579–590.
- Haddouche, R., Delessert, S., Sabirova, J., Neuvéglise, C., Poirier, Y. and Nicaud, J.-M. (2010) Roles of multiple acyl-CoA oxidases in the routing of carbon flow towards beta-oxidation and polyhydroxyalkanoate biosynthesis in *Yarrowia lipolytica*. *FEMS Yeast Res.* **10**, 917–927.
- Harris, E. (2001) *Chlamydomonas* as a model organism. *Annu. Rev. Plant Physiol. Plant Mol. Biol.* **52**, 363–406.
- Hayashi, Y. and Shinozaki, A. (2012) Visualization of microbodies in *Chlamydomonas reinhardtii*. *J. Plant Res.* **125**, 579–586.
- Hayashi, Y., Sato, N., Shinozaki, A. and Watanabe, M. (2015) Increase in peroxisome number and the gene expression of putative glyoxysomal enzymes in *Chlamydomonas* cells supplemented with acetate. *J. Plant Res.* **128**, 177–185.
- Hernández, M.L., Whitehead, L., He, Z., Gazda, V., Gilday, A., Kozhevnikova, E., Vaistij, F.E., Larson, T.R. and Graham, I.A. (2012) A cytosolic acyltransferase contributes to triacylglycerol synthesis in sucrose-rescued *Arabidopsis* seed oil catabolism mutants. *Plant Physiol.* **160**, 215–225.
- Hooks, M.A., Kellas, F. and Graham, I.A. (1999) Long-chain acyl-CoA oxidases of *Arabidopsis*. *Plant J.* **20**, 1–13.
- Hryb, D.J. and Hogg, J.F. (1979) Chain length specificities of peroxisomal and mitochondrial beta-oxidation in rat liver. *Biochem. Biophys. Res. Commun.* **87**, 1200–1206.
- Hu, J., Baker, A., Bartel, B., Linka, N., Mullen, R.T., Reumann, S. and Zolman, B.K. (2012) Plant peroxisomes: biogenesis and function. *Plant Cell*, **24**, 2279–2303.
- Jaworski, J. and Cahoon, E.B. (2003) Industrial oils from transgenic plants. *Curr. Opin. Plant Biol.* **6**, 178–184.
- Kato, J., Yamahara, T., Tanaka, K., Takio, S. and Satoh, T. (1997) Characterization of catalase from green algae *Chlamydomonas reinhardtii*. *J. Plant Physiol.* **151**, 262–268.
- Kaur, N., Reumann, S. and Hu, J. (2009) Peroxisome biogenesis and function. *Arabidopsis Book*, **7**, e0123.
- Kessel-Vigeli, S.K., Wiese, J., Schroers, M.G., Wrobel, T.J., Hahn, F. and Linka, N. (2013) An engineered plant peroxisome and its application in biotechnology. *Plant Sci.* **210**, 232–240.
- Kim, J.J. and Miura, R. (2004) Acyl-CoA dehydrogenases and acyl-CoA oxidases. Structural basis for mechanistic similarities and differences. *Eur. J. Biochem.* **271**, 483–493.
- Klein, A.T.J., van den Berg, M., Bottger, G., Tabak, H.F. and Distel, B. (2002) *Saccharomyces cerevisiae* acyl-CoA oxidase follows a novel, non-PTS1, import pathway into peroxisomes that is dependent on Pex5p. *J. Biol. Chem.* **277**, 25011–25019.
- Kong, F., Yamasaki, T., Kurniasih, S.D., Hou, L., Li, X., Ivanova, N., Okada, S. and Ohama, T. (2015) Robust expression of heterologous genes by selection marker fusion system in improved *Chlamydomonas* strains. *J. Biosci. Bioeng.* **120**, 239–245.
- Kunz, H.-H., Scharnewski, M., Feussner, K., Feussner, I., Flügge, U.-I., Fulda, M. and Gierth, M. (2009) The ABC transporter PXA1 and peroxisomal beta-oxidation are vital for metabolism in mature leaves of *Arabidopsis* during extended darkness. *Plant Cell*, **21**, 2733–2749.
- Laursen, K.J., Willamme, R., Coosemans, N., Joris, M., Kruse, O. and Remacle, C. (2016) Peroxisomal microbodies are at the crossroads of acetate assimilation in the green microalga *Chlamydomonas reinhardtii*. *Algal Res.* **16**, 266–274.
- Lea, W., Abbas, A.S., Sprecher, H., Vockley, J. and Schulz, H. (2000) Long-chain acyl-CoA dehydrogenase is a key enzyme in the mitochondrial beta-oxidation of unsaturated fatty acids. *Biochim. Biophys. Acta*, **1485**, 121–128.
- Ledesma-Amaro, R. and Nicaud, J.-M. (2016) *Yarrowia lipolytica* as a biotechnological chassis to produce usual and unusual fatty acids. *Prog. Lipid Res.* **61**, 40–50.

- Légeret, B., Schulz-Raffelt, M., Nguyen, H.M., Auroy, P., Beisson, F., Peltier, G., Blanc, G. and Li-Beisson, Y. (2016) Lipidomic and transcriptomic analyses of *Chlamydomonas reinhardtii* under heat stress unveil a direct route for the conversion of membrane lipids into storage lipids. *Plant Cell Environ.* **39**, 834–847.
- Li, X., Zhang, R., Patena, W. *et al.* (2016) An indexed, mapped mutant library enables reverse genetics studies of biological processes in *Chlamydomonas reinhardtii*. *Plant Cell*, **28**, 367–387.
- Li-Beisson, Y., Beisson, F. and Riekhof, W. (2015) Metabolism of acyl-lipids in *Chlamydomonas reinhardtii*. *Plant J.* **82**, 504–522.
- Lisenbee, C.S., Heinze, M. and Trelease, R.N. (2003) Peroxisomal ascorbate peroxidase resides within a subdomain of rough endoplasmic reticulum in wild-type *Arabidopsis* cells. *Plant Physiol.* **132**, 870–882.
- Lisenbee, C.S., Lingard, M.J. and Trelease, R.N. (2005) Arabidopsis peroxisomes possess functionally redundant membrane and matrix isoforms of monodehydroascorbate reductase. *Plant J.* **43**, 900–914.
- Marchesini, S. and Poirier, Y. (2003) Futile cycling of intermediates of fatty acid biosynthesis toward peroxisomal  $\beta$ -oxidation in *Saccharomyces cerevisiae*. *J. Biol. Chem.* **278**, 32596–32601.
- Merchant, S.S., Prochnik, S.E., Vallon, O. *et al.* (2007) The *Chlamydomonas* genome reveals the evolution of key animal and plant functions. *Science*, **318**, 245–250.
- Moire, L., Rezzonico, E., Goepfert, S. and Poirier, Y. (2004) Impact of unusual fatty acid synthesis on futile cycling through  $\beta$ -oxidation and on gene expression in transgenic plants. *Plant Physiol.* **134**, 432–442.
- Napier, J.A. (2007) The production of unusual fatty acids in transgenic plants. *Annual Review of Plant Biology* Palo Alto: Annual Reviews, pp. 295–319.
- Nguyen, H.M., Cui, S., Beyly-Adriano, A., Légeret, B., Billon, E., Auroy, P., Beisson, F., Peltier, G. and Li-Beisson, Y. (2013) The green microalga *Chlamydomonas reinhardtii* has a single  $\omega$ -3 fatty acid desaturase that localizes to the chloroplast and impacts both plastidic and extraplastidic membrane lipids. *Plant Physiol.* **163**, 914–928.
- Pinfield-Wells, H., Rylott, E.L., Gilday, A.D., Graham, S., Job, K., Larson, T.R. and Graham, I.A. (2005) Sucrose rescues seedling establishment but not germination of *Arabidopsis* mutants disrupted in peroxisomal fatty acid catabolism. *Plant J.* **43**, 861–872.
- Plancke, C., Vigeolas, H., Hohner, R. *et al.* (2014) Lack of isocitrate lyase in *Chlamydomonas* leads to changes in carbon metabolism and in the response to oxidative stress under mixotrophic growth. *Plant J.* **77**, 404–417.
- Poirier, Y. (2002) Polyhydroxyalkanoate synthesis in plants as a tool for biotechnology and basic studies of lipid metabolism. *Prog. Lipid Res.* **41**, 131–155.
- Poirier, Y., Antonenkov, V.D., Glumoff, T. and Hiltunen, J.K. (2006) Peroxisomal  $\beta$ -oxidation – a metabolic pathway with multiple functions. *Biochim. Biophys. Acta*, **1763**, 1413–1426.
- Poliner, E., Panchy, N., Newton, L., Wu, G., Lapinsky, A., Bullard, B., Zienkiewicz, A., Benning, C., Shiu, S.H. and Farre, E.M. (2015) Transcriptional coordination of physiological responses in *Nannochloropsis oceanica* CCMP1779 under light/dark cycles. *Plant J.* **83**, 1097–1113.
- Pracharoenwattana, I., Cornah, J.E. and Smith, S.M. (2005) Arabidopsis peroxisomal citrate synthase is required for fatty acid respiration and seed germination. *Plant Cell*, **17**, 2037–2048.
- Pracharoenwattana, I., Zhou, W.X. and Smith, S.M. (2010) Fatty acid  $\beta$ -oxidation in germinating Arabidopsis seeds is supported by peroxisomal hydroxypyruvate reductase when malate dehydrogenase is absent. *Plant Mol. Biol.* **72**, 101–109.
- Purdue, P.E. and Lazarow, P.B. (2001) Peroxisome biogenesis. *Annu. Rev. Cell Dev. Biol.* **17**, 701–752.
- Rambold, A.S., Cohen, S. and Lippincott-Schwartz, J. (2015) Fatty acid trafficking in starved cells: regulation by lipid droplet lipolysis, autophagy, and mitochondrial fusion dynamics. *Dev. Cell*, **32**, 678–692.
- Rasala, B.A., Barrera, D.J., Ng, J., Plucinak, T.M., Rosenberg, J.N., Weeks, D.P., Oyler, G.A., Peterson, T.C., Haerizadeh, F. and Mayfield, S.P. (2013) Expanding the spectral palette of fluorescent proteins for the green microalga *Chlamydomonas reinhardtii*. *Plant J.* **74**, 545–556.
- Rhodin, J.A.G. (1954) *Correlation of Ultrastructural Organization: and Function in Normal and Experimentally Changed Proximal Convoluted Tubule Cells of the Mouse Kidney: An Electron Microscopic Study*. Stockholm: Dept. of Anatomy, Karolinska Institutet.
- Shimogawara, K., Fujiwara, S., Grossman, A. and Usuda, H. (1998) High-efficiency transformation of *Chlamydomonas reinhardtii* by electroporation. *Genetics*, **148**, 1821–1828.
- Shinozaki, A., Sato, N. and Hayashi, Y. (2005) Reporter gene assay of targeting signal-like elements and the expression pattern of peroxisomal enzymes in *Chlamydomonas reinhardtii*. *Plant Cell Physiol.* **46**, 823–829.
- Shinozaki, A., Sato, N. and Hayashi, Y. (2009) Peroxisomal targeting signals in green algae. *Protoplasma*, **235**, 57–66.
- Siaut, M., Cuine, S., Cagnon, C. *et al.* (2011) Oil accumulation in the model green alga *Chlamydomonas reinhardtii*: characterization, variability between common laboratory strains and relationship with starch reserves. *BMC Biotechnol.* **11**, 7.
- Sizova, I., Fuhrmann, M. and Hegemann, P. (2001) A *Streptomyces rimosus* aphVIII gene coding for a new type phosphotransferase provides stable antibiotic resistance to *Chlamydomonas reinhardtii*. *Gene*, **277**, 221–229.
- Slocombe, S., Cornah, J., Pinfield-Wells, H., Soady, K., Zhang, Q., Gilday, A., Dyer, J. and Graham, I. (2009) Oil accumulation in leaves directed by modification of fatty acid breakdown and lipid synthesis pathways. *Plant Biotechnol. J.* **7**, 694–703.
- Stabenau, H., Winkler, U. and Saftel, W. (1984) Enzymes of  $\beta$ -oxidation in different types of algal microbodies. *Plant Physiol.* **75**, 531–533.
- Stabenau, H., Winkler, U. and Saftel, W. (1989) Compartmentation of peroxisomal enzymes of the group of *Prasinophyceae* – occurrence of possible microbodies without catalase. *Plant Physiol.* **90**, 754–759.
- Stevens, D.R., Purton, S. and Rochaix, J.D. (1996) The bacterial phleomycin resistance gene as a dominant selectable marker in *Chlamydomonas*. *Mol. Gen. Genet.* **251**, 23–30.
- Tardif, M., Atteia, A., Specht, M. *et al.* (2012) PredAlgo, a new subcellular localization prediction tool dedicated to green algae. *Mol. Biol. Evol.* **29**, 3625–3639.
- Theodoulou, F.L. and Eastmond, P.J. (2012) Seed storage oil catabolism: a story of give and take. *Curr. Opin. Plant Biol.* **15**, 322–328.
- Trentacoste, E.M., Shrestha, R.P., Smith, S.R., Glé, C., Hartmann, A.C., Hildebrand, M. and Gerwick, W.H. (2013) Metabolic engineering of lipid catabolism increases microalgal lipid accumulation without compromising growth. *Proc. Natl Acad. Sci. USA*, **110**, 19748–19753.
- Troncoso-Ponce, M.A., Cao, X., Yang, Z. and Ohlrogge, J.B. (2013) Lipid turnover during senescence. *Plant Sci.* **205–206**, 13–19.
- Vanroermund, C.W.T., Elgersma, Y., Singh, N., Wanders, R.J.A. and Tabak, H.F. (1995) The membrane of peroxisomes in *Saccharomyces cerevisiae* is impermeable to NAD(H) and acetyl-CoA under in vivo conditions. *EMBO J.* **14**, 3480–3486.
- Winkler, U., Saftel, W. and Stabenau, H. (1988)  $\beta$ -oxidation of fatty acids in algae – localization of thiolase and acyl-CoA oxidizing enzymes in 3 different organisms. *Planta*, **175**, 91–98.
- Zones, J.M., Blaby, I.K., Merchant, S.S. and Umen, J.G. (2015) High-resolution profiling of a synchronized diurnal transcriptome from *Chlamydomonas reinhardtii* reveals continuous cell and metabolic differentiation. *Plant Cell*, **27**, 2743–2769.